U. S. Department of Commerce
National Oceanic and Atmospheric Administration
National Weather Service
National Centers for Environmental Prediction

Office Note 475

Impact of Different Satellite Wind Lidar Telescope Configurations on NCEP GFS Forecast Skill in Observing System Simulation Experiments

Zaizhong Ma[*,1,2], Lars Peter Riishojgaard[1,2], Michiko Masutani[1,2,3], John S. Woollen[3,4], G. David Emmitt[5]

[1]*Earth System Science Interdisciplinary Center (ESSIC), University of Maryland, College Park, MD*
[2]*Joint Center for Satellite and Data Assimilation (JCSDA), College Park, MD*
[3]*NOAA/National Centers for Environmental Prediction (NCEP), College Park, MD*
[4]*I.M. Systems Group, Rockville, MD*
[5]*Simpson Weather Associates, Charlottesville, VA*

November, 2013

* Corresponding Author
E-mail: Zaizhong.Ma@noaa.gov

Abstract

The Global Wind Observing Sounder (GWOS) concept, which has been developed by NASA in response to the National Research Council (NRC) Decadal Survey, is expected to provide global wind profile observations with high vertical resolution, precision, and accuracy when realized. The assimilation of Doppler wind *LIght Detection And Ranging* (LIDAR) data anticipated from the GWOS is being conducted as a series of Observing System Simulation Experiments (OSSEs) at the Joint Center for Satellite and Data Assimilation (JCSDA). A companion paper (Riishojgaard et al., 2012) describes the realistic simulation of this lidar wind data and evaluates the impact on global Numerical Weather Prediction (NWP) of the baseline GWOS using a four-telescope configuration to provide independent line-of-sight wind speeds, while this paper sets out to assess the NWP impact of GWOS equipped with alternative paired configurations of telescopes.. The National Centers for Environmental Prediction (NCEP) Gridpoint Statistical Interpolation (GSI) and Global Forecast System (GFS) were used, at a resolution of T382 with 64 layers, as the assimilation system and forecast model, respectively, in these lidar OSSEs. A set of 45-day assimilation and forecast experiments from July 2 to August 15, 2005 have been set up and executed. The same strategies for observational errors discussed in Riishojgaard et al. (2012) were used in this paper.

In this OSSE study, a control simulation utilizing all of the data types assimilated in the operational GSI/GFS system was compared to three OSSE simulations which added lidar wind data from the different configuration of telescopes (one-, two-, and four-looks), respectively. First, the Root-Mean Squared Error (RMSE) of vector wind from analyses is compared against the Nature Run. A significant reduction of the stratospheric RMSE of vector wind analyses is found for all latitudes when lidar wind profiles are used in the assimilation system. The forecast impacts of lidar data on the wind and temperature fields are also presented. In addition, the anomaly correlations (AC) of geopotential height forecasts at 500 hPa were evaluated to compare the control and different GWOS telescope configuration experiments. The results show that the assimilation of lidar data from the GWOS (one-, two-, or four-"look") can improve the NCEP GFS wind and mass field forecasts**.** The addition of the simulated Lidar wind observations leads to a statistically significant increase in AC scores at day five (120h) of approximately 0.3 (for one-look), 0.7 (for two-looks) and 1.4 (for four-looks) in the northern hemisphere, while of approximately 0.9 (for one-look), 1.8 (for two-looks) and 1.8 (for four-looks) in the southern hemisphere. Larger benefits are found in the Southern Hemisphere, although a significant positive impact is also found in the Northern Hemisphere.

1. Introduction

Wind is one of the basic variables describing the state of the atmosphere together with temperature, pressure, and humidity. Global measurements of the wind field are essential for weather prediction, climate change studies, hurricane prediction, and many other meteorological

studies. While the current measurements of atmospheric winds include many kinds of types of observations, from ground stations, buoys, ships, radiosondes, aircraft, ground-based wind profilers, radiometer, scatterometer and cloud tracking satellites, wind measurements are still inadequate in the present global observing system (GOS), and there is still no direct 3-Dimensional (3-D) structure measurement of the wind field throughout the troposphere and lower stratosphere (approximately 0 to 30 km) on a global scale. A lack of wind observations over data sparse areas (i.e., oceans, tropics and the Southern Hemisphere) can result in rather non-uniform errors in Numerical Weather Prediction (NWP) analyses and subsequent forecast failures. Direct observations of wind profiles have been recognized as the most urgently needed observation type for climate studies as well as numerical weather prediction (WMO, 2004).

Space-based Doppler wind LIDAR has been identified as the key technology necessary to meet the global wind profiling requirement (Emmitt, 1987). Coherent Doppler LIDAR is an attractive technique for remote measurement of winds and wind field statistics (Frehlich et al., 2000; Menzies and Hardesty, 1989) and it has become a promising technique for the global measurement of winds using a space-based platform (Baker et al., 1996). Incoherent Doppler LIDAR has also been proposed for global wind measurements (McKay, 1998).

The first space-based Doppler wind lidar, called the Atmospheric Dynamics Mission (ADM-Aeolus, Stoffelen et al., 2005), is scheduled to be launched into a polar orbit by the European Space Agency (ESA) in 2015. ADM is a demonstration mission measuring profiles of single horizontal line-of-sight (LOS) wind components (Marseille and Stoffelen, 2008; Tan and Andersson, 2007) with a priority on the quality rather than quantity of retrieved winds. Because the ADM-Aeolus mission only has one telescope, the 3-D structure of the wind field remains largely unobserved on a global scale.

With the Global Wind Observing Sounder (GWOS), the objective of the concept mission flying in a 400 km polar orbit is to accurately measure the global winds with four telescopes, which would fill this gap in the Global Observing System (Seablom et al., 2008; Kakar et al., 2007). GWOS utilizes both coherent-detection and direct-detection pulsed Doppler wind lidars in a “hybrid” approach to vertically profile horizontal wind vectors from space. Unlike the one-telescope ADM-Aeolus mission, the GWOS is comprised of four telescopes with two of the telescopes pointing forward and two pointing aft oriented 45° from nadir. Therefore greater benefit can be expected to NWP from the GWOS mission than from ADM-Aeolus.

The benefit from the Space-based Doppler wind observations needs to be accurately and fully assessed before the GWOS concept mission is selected to launch. The Observing System Simulation Experiment (OSSE, Arnold et al., 1986) is a well-established method of providing an objective and quantitative evaluation of future observing systems and instruments. Several OSSEs have investigated the impact of global winds using a space-based Doppler lidar (Atlas et al., 2003 and 1997; Rohaly and Krishnamurti, 1993). These OSSEs used a simple description of the data products. A more complete description of the GWOS mission is required to evaluate the impact of these new data products, to perform comparisons with alternative measurements, and to improve the engineering designs and signal processing for future measurements from space.

The lidar OSSEs for the GWOS concept mission began at the National Centers for Environmental Prediction (NCEP) in 2006. The Nature Run is a 13-month forecast from May 2005 to June 2006 produced by the European Centre for Medium-Range Weather Forecasts (ECWMF) at the resolution of T511L91 (approx 40km horizontal resolution and 91 vertical levels, Masutani et al., 2007, Reale et al., 2007). Since the OSSEs mimic the procedures used to analyze global observations for specifying state of the atmosphere, it is very crucial for validating the realism of the OSSE. The validation has been performed by comparing the statistics of results of assimilating the simulated observations for six-weeks compared with the corresponding statistics obtained from assimilating real observations (Riishojgaard et al., 2012). And the agreement between data impacts from the simulated data and corresponding real data is satisfactory. The NCEP Global Data Assimilation System [Gridpoint Statistical Interpolation (GSI)/Global Forecast System (GFS)] was used (Kleist et al., 2009), at a resolution of T382L64 (approx 35km horizontal resolution and 64 vertical levels), as the assimilation system and forecast model in this OSSE system. The impact experiments with simulated lidar wind data from GWOS have been set up and executed. The impact of the four-telescope lidar wind data on NWP has already been investigated (Riishojgaard et al., 2012) and the results show the lidar wind data from GWOS have a significant impact on the anomaly correlations of 500-hPa geopotential heights (an improvement about 1.4% in the Northern Hemisphere and 1.8% in the Southern Hemisphere in the day-5 forecasts).

The GWOS concept mission is comprised of four telescopes, two forward-pointing and two aft-pointing, each oriented nominally ±45° in both azimuth and elevation relative to the spacecraft's velocity vectors. Although the lidar wind impact from GWOS on the NCEP OSSE system has been recently assessed, the performance from the separate telescopes on the GWOS satellite hasn't been evaluated yet. Another point that should be mentioned is that the GWOS with a single telescope can produce lidar observations similar to the ADM mission. It is very useful in exploring the detailed impact from the different telescopes of the GWOS. Hence, as the follow-on OSSE study we first design three lidar experiments: a "one-look" with single telescope (azimuth angle: 45°), a "two-look" with a pair of telescopes (azimuth angles: 45° and 315°) and a "four-look" with two pairs of telescopes (azimuth angles from one pair is 45° and 315°, the other is 135° and 225°) in this paper, then investigate the potential impact of these three experiments on the analyses and forecasts by comparing them against the control, which assimilates all the same observational data as the NCEP operational data sets in 2005. More scientific ideas from this OSSE study are expected before the GWOS concept mission is launched.

The paper is arranged as follows. The model details are presented in Section 2, which also gives the overview of the GWOS concept mission and describes the Nature Run from the European Centre for Medium-Range Weather Forecasts (ECMWF) global model and the lidar data assimilation methodologies in the GSI data assimilation system. Section 3 describes the experimental design for the different pairs of telescopes in the GWOS concept mission, Section 4 shows the preliminary comparison results to assess the GWOS lidar data impact on the analysis and forecast, and Section 5 gives the conclusions and an outlook for further research related to

the GWOS OSSE study.

2. Description of GWOS mission and OSSE system

a. The GWOS Concept Mission

The Global Wind Observing Sounder (GWOS) concept is one of the 15 priority missions recommended for NASA over the next decade in response to the 2007 NRC Decadal Survey for Earth Science (NRC 2007). As the concept mission serving as the user case for our model-driven sensor web operations concept, GWOS would "improve understanding and prediction of atmospheric dynamics and global atmospheric transport" (Kakar et al., 2007). It would achieve these objectives by making "space based direct lidar measurements of vertical profiles of the horizontal wind field to provide a complete global 3-D picture of the dynamical state, clouds permitting and over the oceans for the first time" (Kakar et al., 2007). A simplified description of the GWOS concept mission will be given here.

The GWOS mission flying in a 400 km polar orbit will meet the objectives of the pre-operational NASA demonstration mission. The recommended technological approach is a hybrid Doppler wind lidar which utilizes the complementary capabilities of two Doppler lidar technologies, a coherent Doppler lidar sensing winds from the aerosol backscattered laser signal at a wavelength of 2 microns and a direct detection Doppler lidar sensing winds from the molecular backscattered laser signal at 355 nm (Seablom et al., 2007b). The measurement principle is based on the fact that the Doppler shift of the return from an emitted pulse of monochromatic electromagnetic radiation can be translated into information about the radial velocity of the air at the origin of the return. Only the velocity component aligned with the lidar beam is measured and the observations are, therefore, often referred to as line-of-sight (LOS) winds (Riishojgaard et al., 2004). The GWOS can provide a direct wind measurement with an accurate height assignment and it can provide a relatively uniform horizontal coverage.

b. The Nature Run and observation data simulation

Observing System Simulation Experiments are a powerful tool to assess the potential impact from the GWOS concept mission on the forecast skill of numerical weather prediction for planned or hypothetical future observing systems (Masutani et al., 2007). Simulation experiments use a model-generated proxy for the real atmosphere, commonly called the 'Nature Run (NR)'. The Nature Run used in this lidar OSSE study is a 13-month forecast using cycle 30r1 of ECMWF's Integrated Forecasting System (IFS), forced with daily sea-surface temperature and sea ice, with a high resolution of T511L91 (Andersson and Masutani, 2010). The horizontal resolution is about 40 km and the output is saved every 3 hours. The initial condition is the IFS operational analysis on 12 UTC on 1 May 2005 and the NR ends at 00 UTC on 1 June 2006. The NR was evaluated and very realistic hurricanes and mid-latitude cyclone statistics were reported (Reale et al., 2007). Its cloud distribution is much more realistic than in the previous NR (Masutani et al., 2010). Statistics of the mid-latitude jet were also studied and

found to be realistic. The same strategies for observational errors discussed in Riishojgaard et al. (2012) were used in this paper.

In this GWOS lidar OSSE study, conventional data are simulated based on a 2005-2006 NCEP CDAS usage. Radiance data were simulated using the Community Radiative Transfer Model (CRTM), version 1.2.2. The data distribution is based on real observations during the Nature Run period. Land surface type and vegetation type from the Nature Run were used for this simulation. A data set with no addition of error and a crude assessment of cloud structure has been generated. Detailed information can be found on the Joint OSSE home page (http://www.emc.ncep.noaa.gov/research/JointOSSEs/).

c. LIDAR OSSE system

In these GWOS lidar observing system simulation experiments, the December 2009 (FY10) version of the NCEP GSI/GFS global data assimilation system (Kleist et al., 2009) was used. The experiment setting is consistent with the operational GSI/GFS system at NCEP, except that model resolution of T382L64 has been used rather than the current (April 2012) operational resolution of T574. A short term forecast (6 hours) is run to obtain a first guess for the data assimilation, which uses a ±3 hour data cutoff window, and the analyses and forecasts are centered at 0000, 0600, 1200 and 1800 UTC.

The lidar wind operator has been developed and tested to assimilate the LOS lidar measurements within the GSI data assimilation system. The observation operator for horizontal line-of-sight winds is relatively simple, consisting of an interpolation of the horizontal wind component of the background field to the observation time and location, followed by a projection on the line of sight of the lidar. The analysis is obtained by minimizing the scalar cost function:

(1)

where the vector represents the background or prior estimate of the control vector x, and (analysis state) when minimized; B is the background error covariance matrix; R is the observational and representativeness error covariance matrix; the vector **y** contains the available observations, e.g., lidar wind data in this OSSE; and $H[\mathrm{x}]$ is a the observational operator that transforms from the model state to the observation space as described above.

A key point about this lidar OSSE system is that the Nature Run is performed with ECMWF's Integrated Forecasting System, while the lidar impact experiments are carried out with NCEP GSI/GFS system. So the problem of "identical twins", where the same analysis/forecast system is used, has been avoided in our OSSEs.

3. Experimental Design

To assess the impact of the simulated lidar wind data from the different configurations of telescopes in the GWOS system, two sets of experiments were conducted: first, a cycling assimilation experiment for a 45-day period from 1200 UTC on 1 July to 0000 UTC on 15

August 2005, in which the GSI assimilation system is used for the analysis component and the GFS forecast model is used for the 6-h forecast component. Due to limited computer resources, one forecast per day (only from the corresponding analysis at 0000 UTC with the GFS forecast model) was run out to 120 hours. The details of the experimental design are described as follows.

Four experiments have been carried out in each set:

1) CTRL: A control run in which all the simulated equivalents of observations (both conventional and space-based) used operationally by NCEP in 2005;
2) DWL1: a "one-look" lidar run same as CTRL, but adding GWOS lidar wind data from a single telescope (azimuth angle: 45°);
3) DWL2: a "two-look" lidar run same as CTRL, but adding GWOS lidar wind data from a pair of telescopes (one subsystem with two forward-pointing telescopes, azimuth angles: 45° and 315°);
4) DWL: a "four-look" lidar run same as CTRL, but adding GWOS lidar wind data from two pairs of telescopes (one pair is forward-pointing: 45° and 315°; the other is aft-pointing: 135° and 225°). This is an exactly same DWL experiment which had been showed in our companion paper (Riishojgaard et al., 2012).

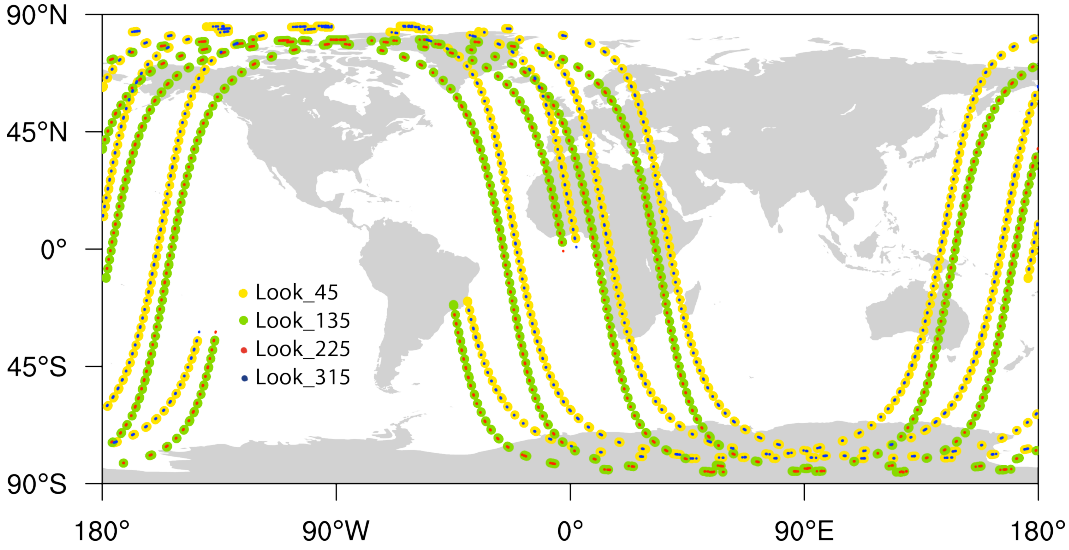

Fig. 01. Number of observations in the 6-hour assimilation window at the analysis time 0000 UTC 21 July 2005. (from Riishojgaard et al., 2012)

In this OSSE, the initial analysis assimilating all the data types same as the NCEP operational observation set in 2005 was utilized as the control run. In order to determine what the different configurations of GWOS wind observations contribute to skill, we also ran and diagnosed the following data denial experiments: one-look, two-look or four-look lidar data were added on top of the control. The number of observations in the 6-hour assimilation window at the analysis time 0000 UTC 21 July 2005 is shown in Figure 1. Figure 2 shows a comparison of the lidar data counts from these three lidar runs within the ±3 hour assimilation window, initialized at 0000 UTC from 2 July to 15 August 2005, before/after the quality control procedure of the

GSI system. It is clear that the distribution of GWOS lidar data counts (for one-, two- or four-look runs) is very stable with time in the cycling experiment. About 7,500 lidar data points are assimilated within the 6-h assimilation window for the one-look run. The data volume from the two-look run is about double the size of the one-look run, and the same thing happens when comparing the four-look and two-look runs.

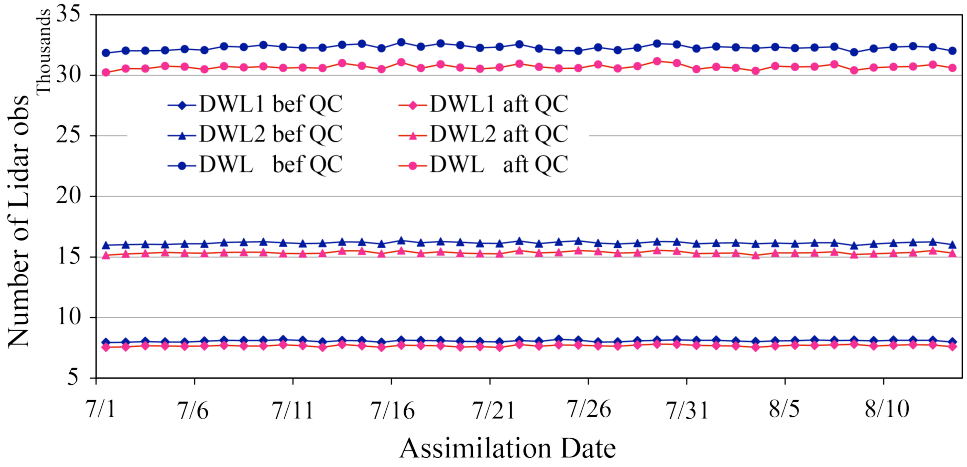

Fig. 02. A comparison of the lidar data counts from DWL1 (one-look), DWL2 (two-look) and DWL (four-look) runs before/after quality control in the GSI system. Statistics for each run were initialized at 0000 UTC within a ±3 hour assimilation window each day from 2 July to 15 August 2005. About 6% of the lidar data is rejected by the quality control procedure in the GSI.

4. Preliminary Results

The observation system simulation experiments were conducted to compare the respective impacts of using the simulated lidar data from the different pairs of telescopes on the GWOS concept mission. The preliminary results are analyzed in this section as follows. First, we discuss the impact of the different sets of lidar wind data on analyses for the complete 45-day assimilation period. In the second subsection, we perform the 120-h forecasts where the analysis from each run serves as the forecast initial state. The impact of lidar data on forecasts is assessed based on the different configurations and using some objective statistical measures to verify forecasts initialized with (DWL1, DWL2 and DWL) and without (CTRL) lidar data. In this OSSE, forecast impact comparisons will be presented for assimilating the operational data to a benchmark or Control experiment. The impact on the quality of the GFS forecasts from assimilating the different sets of lidar data is explored in detail.

The primary fields used for the verification are the tropical winds and the extratropical 500-hPa geopotential heights. Several objective statistical measures to verify forecast quality are commonly used. Most popular among these are the Root-Mean Squared Error (RMSE) and the Anomaly Correlation Coefficient (ACC) of forecasts against verifying analyses. In these assessments, both analyses and forecasts are verified against the Nature Run for each experiment, using the NCEP operational verification package. The Nature Run from the ECWMF was performed at a resolution of T511L64 and the lidar OSSE was carried out at a

resolution of T382L64.Both datasets were reduced to a 2.5° by 2.5° horizontal resolution before calculating the RMSE and anomaly correlations with this package. The extratropical verification is done for the latitudinal bands of 20°-80° in each hemisphere, while the tropical verification is done in the band from 20°N to 20°S. More details about the NCEP verification package can be found on the NCEP web site (http://www.emc.ncep.noaa.gov/gmb/STATS_vsdb/).

a. Comparison of the Analysis Impact

In this section, the comparison of vector winds from analyses with respect to the Nature Run is investigated first. Here RMSE is defined according to the WMO standard using the following equation:

(2)

where F is the analysis or forecast value of the parameter under investigation, A is the true atmospheric state (from the Nature Run), and N is the total number of points in a temporal or spatial domain or a spatial-temporal combined space. The summation is over all gridpoints inside the verification area. In the case of wind vector verification, the summation in the numerator contains two terms - the zonal and the meridional wind components.

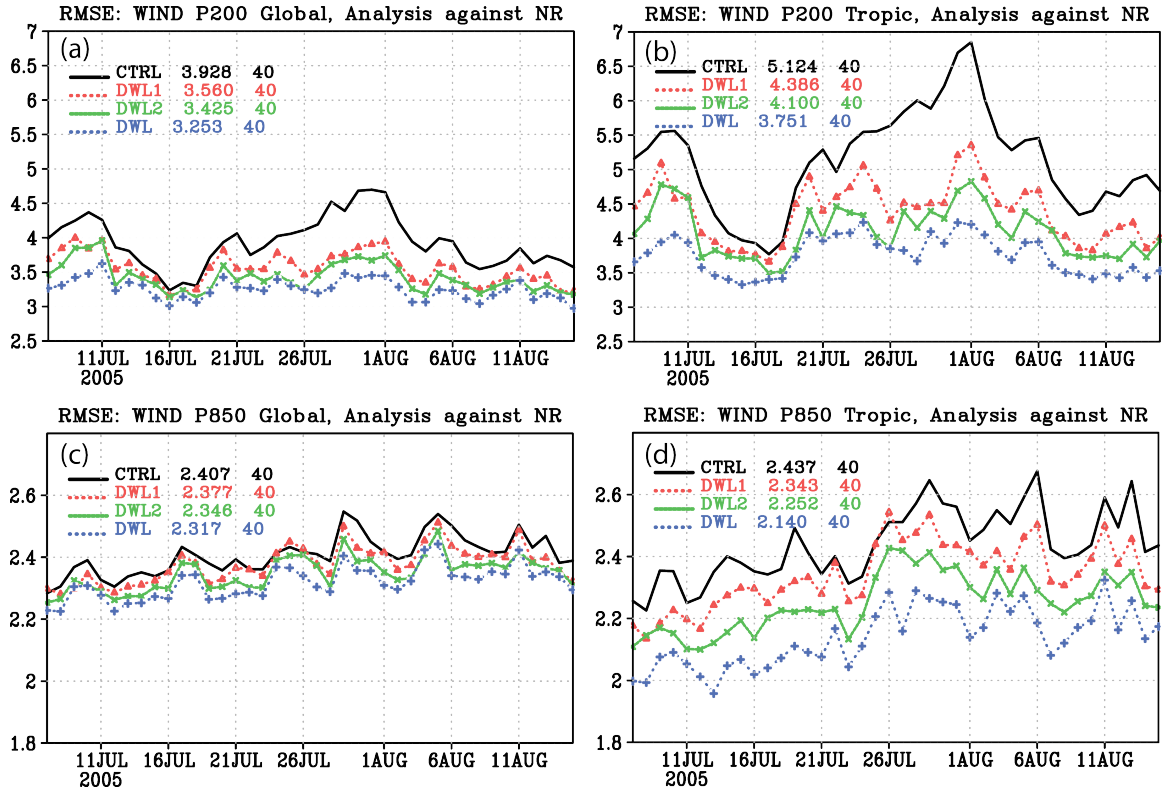

Fig. 03. Time series of the vector wind RMSE at (a, b) 200 hPa and (c, d) 850 hPa for analyses verifying daily from 7 July through 15 August 2005 in the (a, c) Global and (b, d) Tropical regions. Analyses for each run were initialized at 0000 UTC and verified against the Nature Run.

CTRL (black) = control run; DWL1 (red) = one-look run; DWL2 (green) = two-look run; and DWL (blue) = four-look run.

A time series of RMSE from the wind vector analysis is displayed in Figure 3 for different pressure levels and regions of the globe, i.e., Fig. 3b presents a comparison of wind vector RMSE for four OSSE experiments (CTRL, DWL1, DWL2 and DWL) at 200 hPa over the tropical regions. Compared with the CTRL, a positive impact from lidar data on the analysis is clearly seen. The temporal mean, taken over all 40 cases displayed, is shown in the middle column of the legend in each figure. In order from worst to best, the time-averaged RMS error of the tropical 200 hPa winds of the four experiments are: CTRL (5.124 ms^{-1}) > DWL1 (4.386 ms^{-1}) > DWL2 (4.100 ms^{-1}) > DWL (3.751 ms^{-1}). Similar results can be found at 850 hPa (Fig. 3d) and in the globe (Figs. 3a and 3c). Not surprisingly, a larger impact from lidar data on the analysis is clearly seen in the tropics than globally, because of the reduced coverage of observational data over the ocean in the tropics. A smaller but consistently beneficial impact is found in the Northern Hemisphere (not shown) as well.

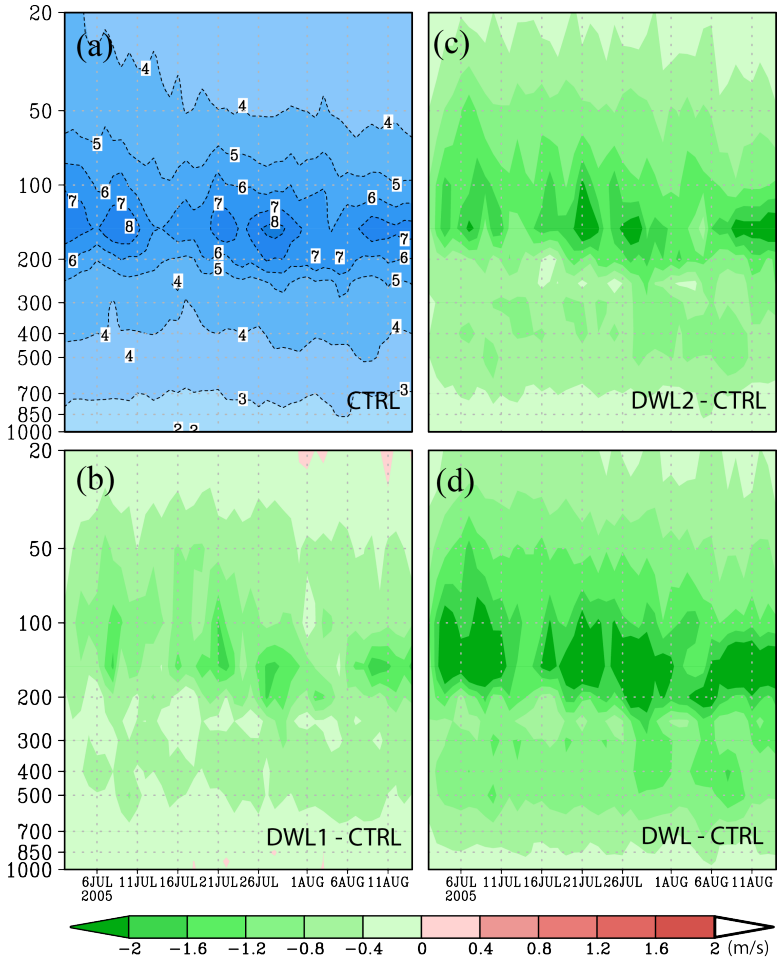

Fig. 04. The RMSE comparison of tropical vector wind analyses over the complete assimilation period. (a) Time series of tropical wind RMSE from CTRL against Nature Run for each pressure level (from 1000 hPa to 20 hPa). (b), (c) and (d) show the difference between the RMSEs of

lidar (DWL1, DWL2 or DWL) and CTRL runs, respectively. Red areas denote a negative lidar impact, green areas a positive impact. It is clearly to show the biggest impact of lidar observations is in the higher level (between 200 and 50 hPa).

Figure 4 shows the time-height distribution of RMSE from the wind vector analysis against the Nature Run for pressures from 1000 hPa to 20 hPa in the tropics. The biggest RMSE value from the CTRL run (Fig. 4a) appears at the higher altitudes between 200 to 50 hPa. The differences between the lidar runs (DWL1, DWL2 and DWL) and the CTRL are calculated and shown in Figs. 4b-4d. The green areas denote a positive impact of the wind lidar observations, or in other words, the wind vector RMSE from the lidar run is smaller than that from the CTRL. On the other hand, red areas denote a negative impact of the lidar data. It is clearly seen that most areas are positively affected. The largest positive impact of the lidar data appears at the higher altitudes for each lidar experiments, and DWL run assimilating the four-look GWOS observations can produce the largest impact on the analyses in these three lidar experiments.

b. Comparison of the Forecast Impact

To compare the impact of GWOS lidar data from the different configurations of telescopes on the 120-h forecasts, four experiments (CTRL, DWL1, DWL2 and DWL) have been performed, initializing with the 0000 UTC analyses from 2 July to 15 August 2005. In the 120-h forecast impact diagnostics, the first few days of each run were removed from these results to allow the assimilation system and forecast model to adjust to the new data. A total of 40 cases were taken to verify against the Nature Run in this OSSE, i.e., 120-h forecasts from 7 July to 15 August 2005. Differences between the forecasts from the four parallel runs are only due to the impact of the simulated GWOS lidar data. Hence, their respective quality is a measure of observation impact.

1) TROPICAL WIND

As an example of GWOS lidar impact on the forecast, Figure 5 presents the time series of vector wind RMSE at day 3 against the Nature Run for pressures from 1000 hPa to 20 hPa in the tropics. A zonal belt of the biggest vector wind RMSE from the CTRL appears between 200 and 50 hPa, and the central value of the wind is more than 11 ms^{-1}. The differences between the three lidar runs and CTRL are shown in Figs. 5b-5d. Compared to the CTRL, it's clearly seen that all of three lidar runs can decrease the wind vector forecast RMSE after the GWOS lidar observations are assimilated, and the biggest benefit from the lidar observations still appear at the higher altitudes. During these three lidar runs, DWL1 (only assimilating one-look GWOS data) produces the smallest positive impact on the day 3 forecast, while the DWL run assimilating the four-look GWOS data can produce the biggest impact.

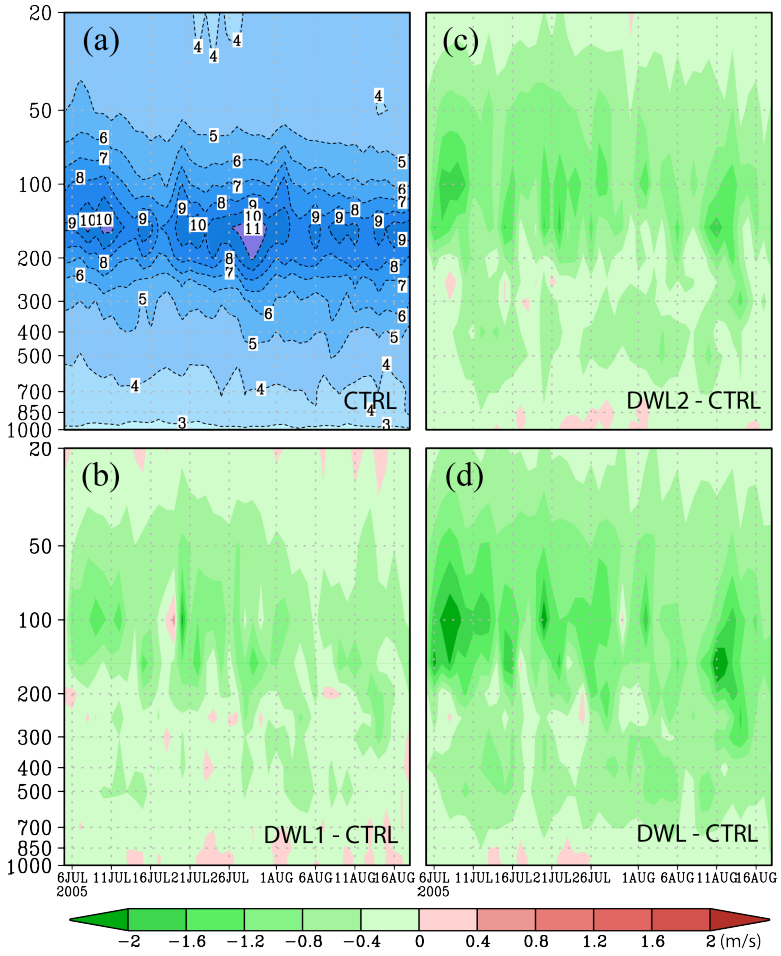

Fig.05. As in Fig. 04, but for the Day-3 forecast vector wind RMSE comparison.

In order to illustrate the wind lidar impact at different forecast ranges, vector wind RMSEs of the forecasts from these four runs versus the Nature Run at 200 and 850 hPa are shown for the tropics in Figure 6. The mean is calculated based on all 40 cases at 0000 UTC each day. The values of vector wind RMSE are shown in the upper panels of each figure, and the differences from the CTRL are shown in the lower panel of each figure. Time 0 represents the analysis. At the 200-hPa pressure level (Fig. 6a), the benefit from the GWOS lidar observations is readily apparent. Wind lidar observations from DWL reduce the tropical wind RMSE by values ranging from 1.4 down to 0.2 ms^{-1}, depending on the range, while the corresponding reductions due to the lidar observations from the others (DWL1 and DWL2) lie between. Similar results are found at the 850-hPa pressure levels, albeit with somewhat less pronounced error reductions.

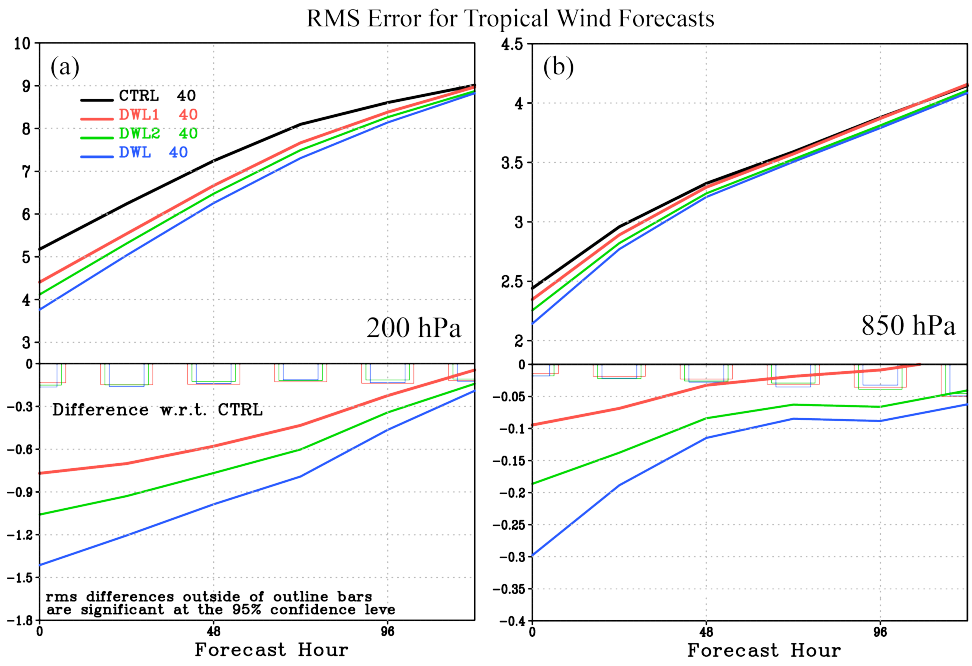

Fig. 06. The vector wind RMSE (m/s) by forecast time for CTRL (black), DWL1 (red, one-look), DWL2 (green, two-look) and DWL (blue, four-look) forecasts verifying daily from 7 July through 15 August 2005 in the tropics at (a) 200 hPa and (b) 850 hPa. In the lower panel of each figure, the error bars represent the significance of the difference between the lidar (DWL1, DWL2 and DWL) and CTRL runs at the 95% confidence level. Forecasts for each run were initialized at 0000 UTC and verified against the Nature Run.

Besides 200 and 850 hPa, the performance comparison of lidar impact for all pressure levels is also investigated in Figure 7. The green color dominates in Figs. 7b-7d and the largest positive impact from lidar is located around 150 hPa.

Overall, the comparison of vector wind RMSE differences in the tropics (Figures 5-7) shows that the experiments assimilating GWOS lidar data show greatly improved vector wind RMSE statistics compared to the CTRL. The largest lidar benefits appeared at the upper levels, for all three lidar runs, while the four-look DWL can produce the largest positive impact on the vector wind forecast, followed by DWL2 (two-look) and DWL1 (one-look) lidar configurations.

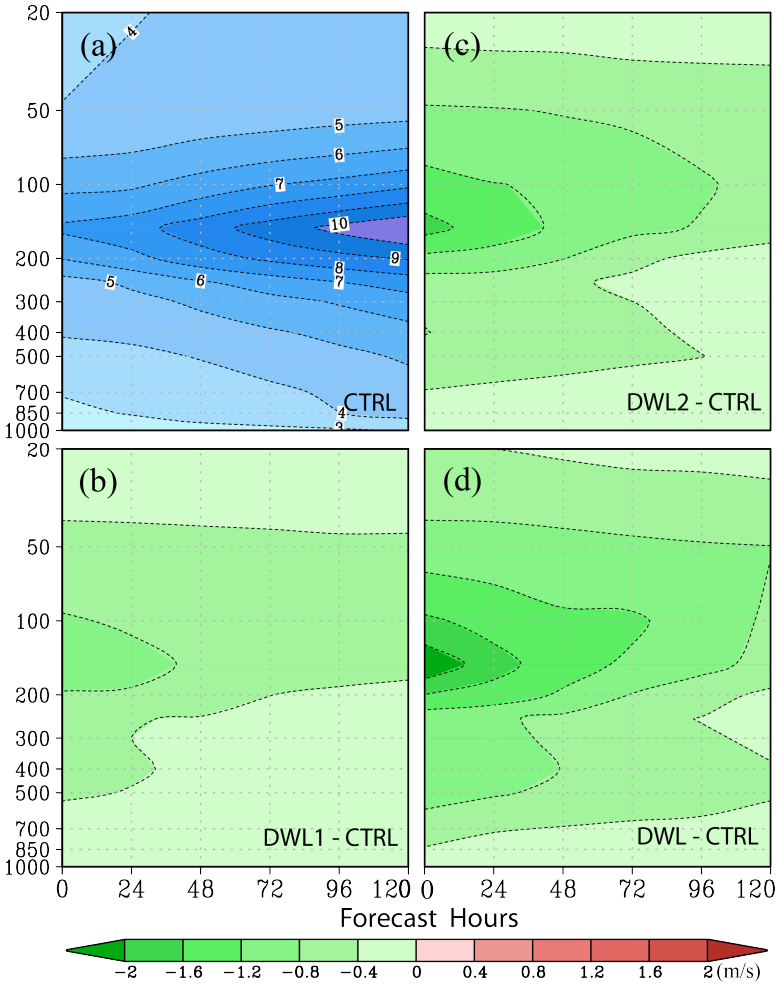

Fig. 07. The RMSE comparison of forecast tropical vector wind at 120-hours verifying daily 0000 UTC from 7 July through 15 August 2005. (a) Tropical wind RMSE with the forecast time from CTRL against Nature Run for each pressure level (from 1000 hPa to 20 hPa). (b), (c) and (d) show the difference with the forecast time between the RMSEs of lidar (DWL1, DWL2 or DWL) and CTRL runs, respectively. Red areas denote a negative lidar impact, green areas a positive impact. It clearly shows the biggest impact of lidar observations is at the higher levels (between 200 and 50 hPa). The interval is 0.4 ms^{-1}.

2) TEMPERATURE

The lidar wind observations from the GWOS concept mission do not contain direct information on the mass field, meaning that we can not obtain mass increments in the analysis through the adjoint of the forward operator for lidar wind in the GSI data assimilation system. The increments for the mass components due to the lidar wind data, if any, should come through the dynamics of the model and the balance constraints in the GSI. In general, we found neutral or slightly positive impacts for the temperature when GWOS lidar data was included in the GSI assimilation system. This can be seen in Figure 8, where the 700-hPa RMSE for temperature with forecast time is displayed for these four experiments in the Northern and Southern hemispheres. The verification is done against the Nature Run discussed above. The forecast impact of GWOS lidar after 72 hours was quite clear for the period being tested.

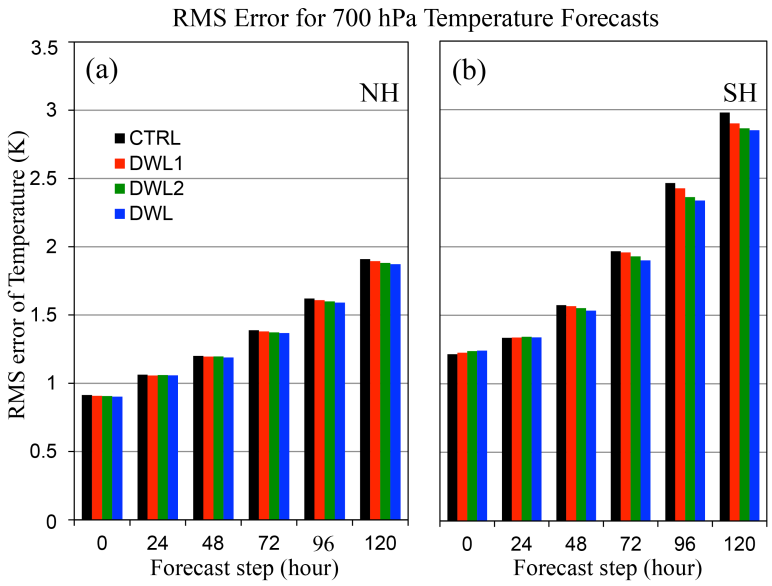

Fig. 08. 700 hPa RMS forecast error comparison for temperature averaged over the period from 7 July to 15 August 2005 in the (a) Northern and (b) Southern Hemispheres. Forecast error is defined as the forecast minus the true atmospheric state from the Nature Run. Forecasts for each run were initialized with analyses at 0000 UTC each day.

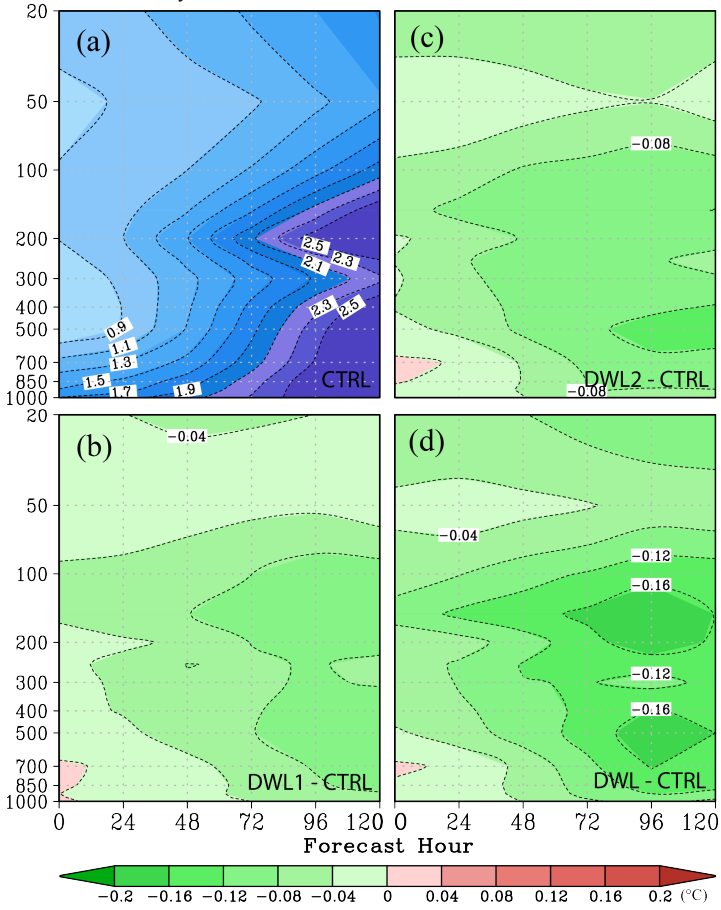

Fig. 09. As in Fig. 07, but for the comparison of temperature RMSE in the Southern Hemisphere. The interval is 0.04°C.

To compare fully with the temperature forecasts, RMSE from the CTRL and differences with the other three lidar runs for all pressure levels are presented in Figure 9 for the Southern Hemisphere. While the green color (in Fig. 9b) still dominates at most pressure levels, the difference from DWL1 is very small and much close to neutral. On the other hand, there have two areas of big positive lidar impact on forecasts from DWL2 (in Fig. 9c) and DWL (in Fig. 9d), where the decrease in central value from the CTRL is about 0.1°C at day 4.

3) GEOPOTENTIAL HEIGHT ANOMALY CORRELATION

In addition to the tropical winds and temperature, the Anomaly Correlation Coefficients (ACC) for the geopotential height fields at 500 hPa in the extratropics was calculated using the NCEP verification package. The anomaly correlation is defined as the correlation between the forecast and analyzed deviations (anomalies) from climatology (Holton, 1992). The following expression is used for computing the anomaly correlation of geopotential height at 500 hPa:

(3)

Here the suffix F denotes the forecast, C denotes climatology, and V indicates verification data (the Nature Run for these experiments). The over-bar indicates the areal mean and Z is the geopotential height at 500hPa. The summations in this equation are made over space.

Figure 10 displays time series of 500-hPa geopotential height anomaly correlation at day 5 in the Northern and Southern hemispheres. Values from all four experiments (CTRL, DWL1, DWL2 and DWL) remain above 0.8 except during the first few days in the Northern Hemisphere (Fig. 10a) and above 0.7 for most days in the Southern Hemisphere (Fig. 10b). The means in the middle column of the legend for each panel are taken over all cases initialized at 0000 UTC during the whole forecast period, and its sequence in NH is: CTRL (0.849) < DWL1 (0.852) < DWL2 (0.856) < DWL (0.864). Similar results can be found in SH as well. Specially, the large positive impact can be found some days, i.e., July 20 in NH and August 5 in SH.

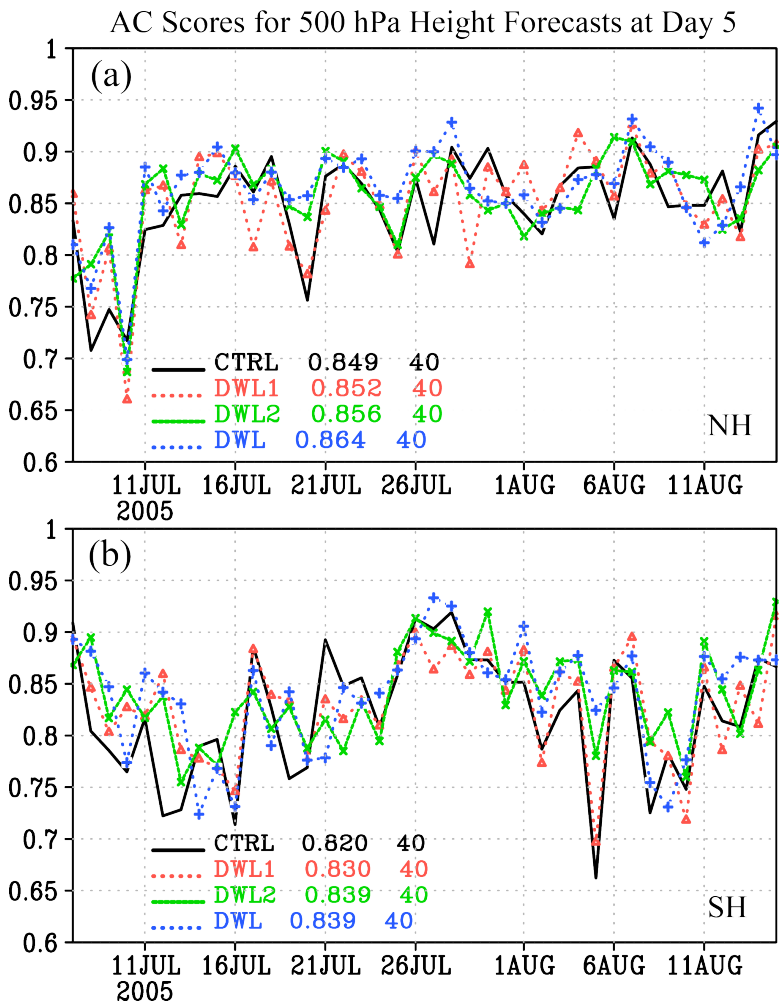

Fig. 10. Time series of the 500-hPa geopotential height anomaly correlation scores on Day 5 for CTRL (black), DWL1 (red, one-look), DWL2 (green, two-look) and DWL (blue, four-look) forecasts verifying daily from 7 July through 15 August 2005 in the (a) Northern and (b) Southern Hemispheres. Forecasts for each run were initialized at 0000 UTC and verified against the Nature Run.

With this study, it was hoped to detect some kind of transient feature which reduces a large error field and the resulting positive impact on 500-hPa geopotential height forecast after assimilating the lidar wind observations from the GWOS. To accomplish this, a subset of the good Day-5 forecast cases from DWL (four-look experiments) in the southern hemisphere on August 5 was studied. The error field evolution for this specific high impact case is shown in Fig. 11. This figure shows the daily evolution of the 500-hPa geopotential height forecast difference between CTRL and DWL experiments as forecast from the initial conditions in CTRL run which produced the poor 5-day forecast valid 5 Aug 2005. Visual inspection of these three forecast error fields reveals that there are significant changes in the locations of major errors for the forecast valid date at the five forecast lengths. There were noticeable differences in the amplitudes of the error centers.

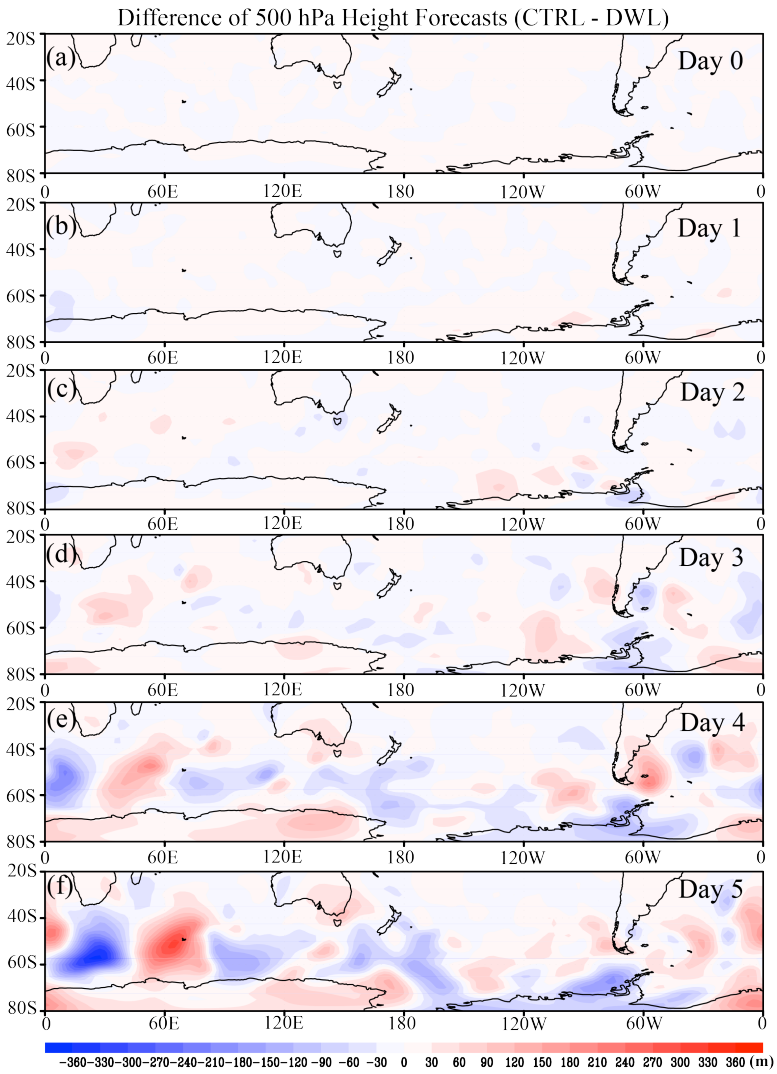

Fig. 11. Daily 500-hPa geopotential height forecast difference between CTRL and DWL experiments evolving from the initial conditions which produce a poor 5-day forecast from CTRL valid August 5th, 2005 in South Hemisphere showed in Fig. 10b. (a.) day 0, (b.) day 1, (c.) day 2, (d.) day 3, (e.) day 4 and (f.) day 5 height forecast difference. Contour interval is 30 meters.

In addition to the study of error growth described above, the magnitude of lidar benefit from GWOS was examined with the equation as abs(CTRL-NR) minus abs(DWL-NR) in Figure 12. The valid date is the same as the case shown in Fig.11. The red area denotes a positive impact of the wind lidar observations, in other words, the forecast error from DWL against NR is smaller than that from CTRL. On the other hand, blue area is bad and lidar wind observations have negative impact on the model forecast. The lidar positive impact becomes stronger with forecast time.Red color can be clearly seen in most of the south hemisphere, especially over the ocean to the south of Africa. The 5100m height line of GWOS DWL experiments at day 5 is much closer to the NR than that of the CTRL.

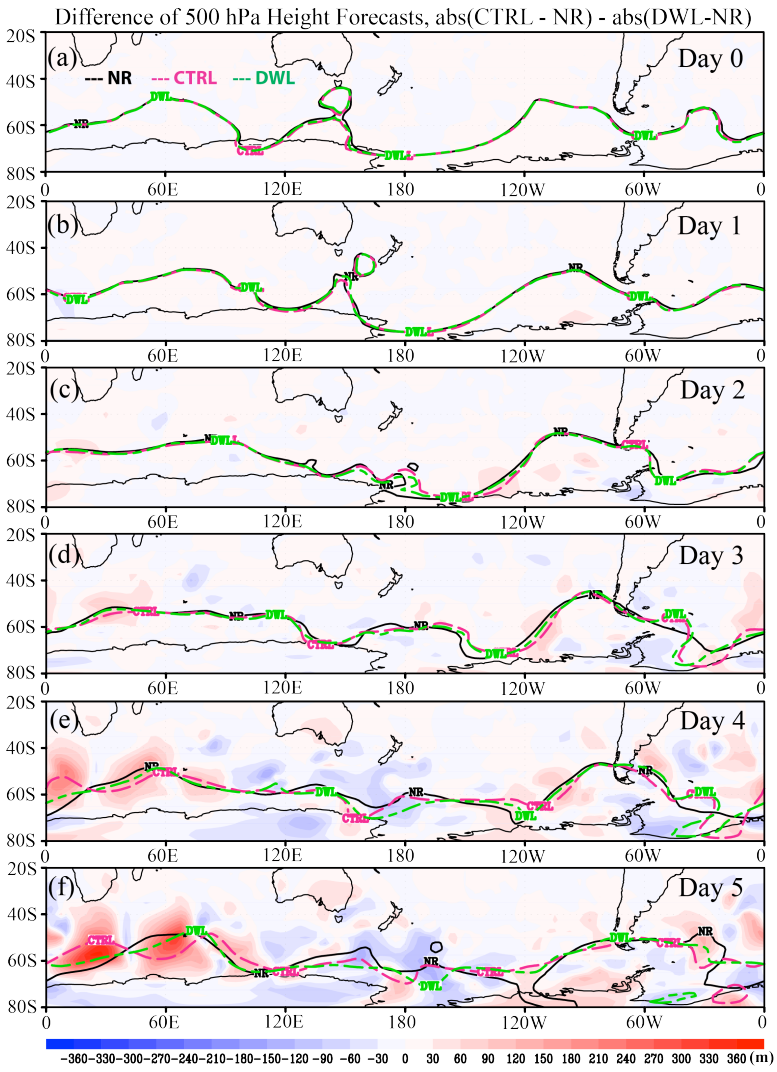

Fig. 12. Same as Fig. 11, but for two experiments (CTRL and DWL) against nature run (NR). The equation is abs(CTRL-NR) – abs(DWL-NR). Red Area denotes that forecast error from DWL against NR is smaller than CTRL, it's good and Lidar data produce positive impact on the model forecast. On the other hand, blue area is bad and Lidar have negative impact on the model forecast. 5100m height shows in three curves (Black line: NR; Purple long-dash: CTRL; and Gree short-long-dash: DWL).

In Figure 13, anomaly correlations of 500-hPa geopotential height from all four OSSE 120-h forecasts are compared for the Northern and Southern hemispheres, respectively. The increase of AC skill in the three lidar runs over the CTRL is more significant in the SH (Fig. 12b) than in the NH.The benefits of lidar are already noticeable in the SH at short-range forecasts (day 2) and increase with forecast time. The addition of the simulated Lidar wind observations leads to a statistically significant increase in AC scores at day five (120h) of approximately 0.3 (for one-look), 0.7 (for two-looks) and 1.4 (for four-looks) in the northern hemisphere, while of approximately 0.9 (for one-look), 1.8 (for two-looks) and 1.8 (for four-looks) in the southern hemisphere. Although the impacts from these lidar runs in the NH are less significant than in the SH, the results are still encouraging.

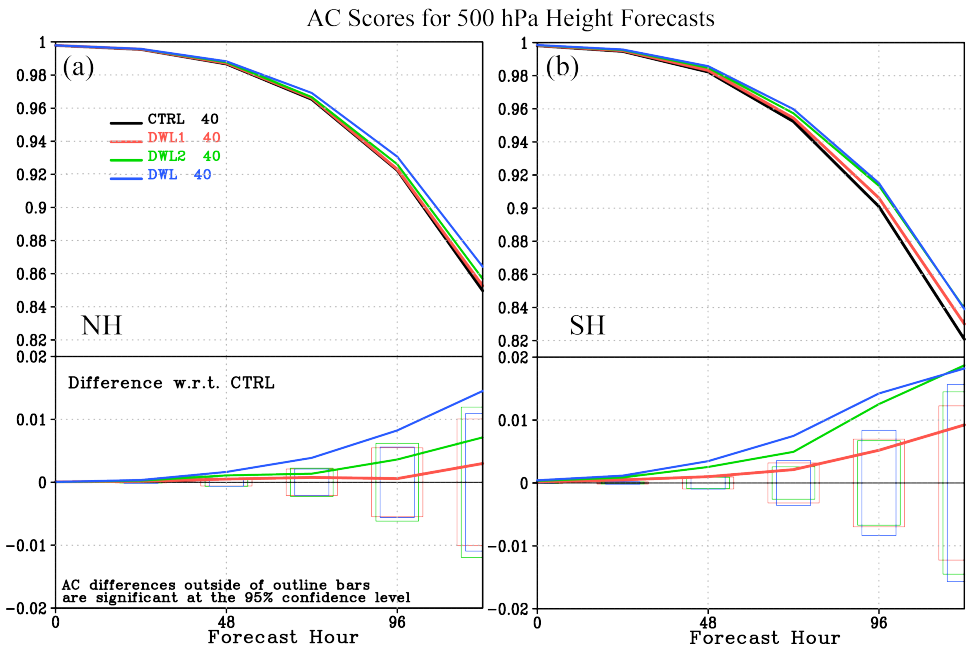

Fig. 13. The average 500-hPa geopotential height anomaly correlation scores by forecast time for CTRL (black), DWL1 (red, one-look), DWL2 (green, two-look) and DWL (blue, four-look) forecasts verifying daily from 7 July through 15 August 2005 in the (a) Northern and (b) Southern Hemispheres. In the lower panel of each figure, the error bars represent the significance of the difference between the lidar (DWL1, DWL2 and DWL) and CTRL runs at the 95% confidence level. Forecasts for each run were initialized at 0000 UTC and verified against the Nature Run.

5. Summary and future plans

Observing system simulation experiments are important for understanding the impact of new data on NWP forecasts. The wind lidar observation from GWOS is one of the most promising sources of satellite sounding data for operational numerical weather prediction in the future. The lidar impacts from the different GWOS lidar wind configurations have been investigated through a set of the observing system simulation experiments performed with a 2009 version of the NCEP GSI/GFS System. Four separate OSSE experiments (CTRL, DWL1, DWL2 and DWL) were run in order to compare forecast skill with and without GWOS wind lidar data at a resolution of about 35km. First, each experiment performed data assimilation cycling experiments with a 6-h assimilation window over a six-week period from 1 July to 15 August 2005. Then 5-day forecasts were carried out using the analyses performed from the 00z-cycle each day.

Analyses and forecasts from the four OSSE runs were verified against the Nature Run using the NCEP operational verification package. The results indicate that assimilation of the GWOS lidar data (one-, two-, or four-looks) can substantially improve the NCEP GFS wind and mass forecasts**.** Larger benefits can be found in the Southern Hemisphere, although a significant positive impact is also found in the Northern Hemisphere. The GWOS lidar observations with four-look configuration (DWL) have larger impact on both analyses and forecasts than the observations from the other two lidar configurations (DWL1 or DWL2). Additional diagnostics for specific high impact case is performed to examine the growth of forecast error. This

examination reveals the dominant modes of error growth, both in time and space. Additionally, it reveals differences between the dominant modes of poor and good forecasts with/without DWL lidar observations.

This OSSE study demonstrated the potential benefits of adding space-based GWOS wind lidar observations on top of the data currently used by NCEP for operational numerical weather predictions. Future work in this area is envisaged to evolve as follows: 1) extending the simulations over the remainder of the simulated 2005 hurricane season; 2) conducting separate assessments of the impacts of Direct Detection and Coherent Detection; 3) determining the impact on applications other than NWP, e.g., chemical transport models; 4) determining the impact of and methodology for observation error assignment.

Acknowledgments

Support for this work was provided by NASA (R. Kakar) through ROSES (grant no. NNX08AQ44G). Computational resources for the experiments were made available by NOAA/NCEP. The T511NR was produced by Dr. Erik Andersson of the ECMWF. Initial simulation of GOES radiance data was conducted by Tong Zhu of NESDIS. We acknowledge Dr. Fanglin Yang for his support about the NCEP verification package and providing valuable comments. The manuscript was significantly improved by addressing the comments by Dr. James G. Yoe.

References:

Andersson, E. and M. Masutani 2010: Collaboration on Observing System Simulation Experiments (Joint OSSE), *ECMWF News Letter* No. **123**, Spring 2010, 14-16.

Arnold, C. P. Jr. and Dey, C. H., 1986: Observing-Systems Simulation Experiments: Past, Present, and Future. *Bull. Amer. Meteorol. Soc.*, **67,** 687–695

Atlas, R., 1997: Atmospheric observation and experiments to assess their usefulness in data assimilation, *J. Meteorol. Soc. Jpn.,* **75**, 111–130.

Becker, B. D., H. Roquet, and A. Stoffelen, 1996: A simulated future atmospheric observation database including ATOVS, ASCAT, and DWL, *Bull. Am. Meteorol. Soc.*, **77**, 2279–2294.

Emmitt, G. D., 1987: Error analysis for total wind vector computations using one component measurements from a space-based Doppler lidar. *Proc. Optical Society of America's Fourth Conf. on Coherent Laser Radar: Technology and Applications,* Aspen, CO, Optical Society of America, 217–220.

Frehlich, R. G., 2000: Simulation of coherent Doppler LIDAR performance for space-based platforms. *J. Appl. Meteor.,* **39,** 245–262.

Kakar, R., Neeck, S., Bajpayee, J., Shaw, H., Gentry, B., Kavaya, M., Sing, U., 2007: "Overview

of An Advanced Earth Science Mission Concept Study for a Global Wind Observing Sounder"; Study slides.

Kleist, Daryl T., David F. Parrish, John C. Derber, Russ Treadon, Wan-Shu Wu, Stephen Lord, 2009: Introduction of the GSI into the NCEP Global Data Assimilation System. *Wea. Forecasting*, **24**, 1691–1705.

Marseille, G. J., A. Stoffelen, and J. Barkmeijer, 2008: Impact assessment of prospective space-borne Doppler wind LIDAR observation scenarios, *Tellus*, Ser. A, 60, 234–248.

Masutani, M, J.S. Woollen, S. J. Lord, G. D.Emmitt, T. J. Kleespies, S. A. Wood, S. Greco, H. Sun, J. Terry, V. Kapoor, R.Treadon, K. A. Campana, 2010: Observing system simulation experiments at the National Centers for Environmental Prediction, *J. Geophys. Res.*, **115**, D07101, doi:10.1029/2009JD012528.

Masutani, M., and Coauthors, 2007: Progress in Observing Systems Simulation Experiments (a new nature run and International collaboration) Preprints, 18th Conference on Numerical Weather Prediction,; AMS confernce Proceeding; Parkcity UT, *Amer.Meteor. Soc.* 12B.5. [Available online at http://ams.confex.com/ams/pdfpapers/124080.pdf]

McKay, J. A., 1998: Modeling of direct detection Doppler wind LIDAR. I. The edge technique. *Appl. Opt.,* **37,** 6480–6486.

Menzies, R. T., and R. M. Hardesty, 1989: Coherent Doppler LIDAR for measurements of wind fields. *Proc. IEEE,* **77,** 449–462.

National Research Council (NRC), 2007: "Earth Science and Applications from Space: National Imperatives for the Next Decade and Beyond," The National Academies Press, Wash DC 2005, "Decadal Survey (DS)."

Reale, O., J. Terry, M. Masutani, E. Andersson, L.P. Riishojgaard & J.C. Jusem, 2007: Preliminary evaluation of the European Centre for Medium-Range Weather Forecasts' (ECMWF) Nature Run over the tropical Atlantic and African monsoon region. *Geophys. Res. Lett.*, **34**, L22810, doi:10.1029/2007GL031640.

Riishojgaard, L. P., Z. Ma, M. Masutani, J. S. Woollen, G. D. Emmitt, S. A. Wood, and S. Greco (2012), Observation system simulation experiments for a global wind observing sounder, *Geophys. Res. Lett.,* 39*, L17805, doi:*10.1029/2012GL051814.

Riishojgaard, L. P., R. Atlas, and G. D. Emmitt, 2004: The impact of Doppler lidar wind observations on a single-level meteorological analysis. *J. Appl. Meteor.,* **43,** 810–820.

Rohaly, G. D., and T. N. Krishnamurti, 1993: An observing system simulation experiment for the laser atmospheric wind sounder (LAWS), *J. Appl. Meteorol.*, **32**, 1453–1471.

Seablom, M., S.J. Talabac, J. Ardizzone and J. Terry, 2008: A Sensor Web Simulator for Design of New Earth Science Observing Systems. *IGARSS(5),* 298-301.

Seablom, M., Talabac, S., Higgins, G., and Womack, B., 2007: Simulation for the Design of Next-Generation Global Earth Observing Systems, *Proc. SPIE Int. SOc. Opt. Eng.* 6684 668413-5

Stoffelen, A., G. J. Marseille, F. Bouttier, D. Vasiljevic, S. De Haan, and C. Cardinali, 2006: ADM-Aeolus Doppler wind LIDAR observing system simulation experiment, *Q. J. R. Meteorol. Soc.*, **619**, 1927–1948.

Stoffelen, A., et al. 2005: The atmospheric dynamics mission for global wind field measurement, *Bull. Am. Meteorol. Soc. Am.*, **86**, 73–87.

Tan, D. G. H., E. Andersson, M. Fisher, and L. Isaksen, 2007: Observing system impact assessment using a data assimilation ensemble technique: Application to the ADM-Aeolus wind profiling mission, *Q. J. R. Meteorol. Soc.*, **133**, 381–390.

World Meteorological Organization (WMO), 2004. Third WMO Workshop on the Impact of Various Observing Systems on Numerical Weather Prediction, Alpbach, Austria, 9–12 March 2004. WMO Proceedings TD 1228.